OPTIMAL ESTIMATION OF ELECTRODE GAP DURING VACUUM ARC REMELTING

Rodney L. Williamson[†], Joseph J. Beaman[‡], Christopher L. Hysinger[‡], and David K. Melgaard[†]

[†]Liquid Metals Processing Laboratory

Sandia National Laboratories

Albuquerque, New Mexico 87185-1134

[‡]Mechanical Engineering Department

University of Texas

Austin, Texas 78712

DISCLAIMER

ABSTRACT

Electrode gap is a very important parameter for the safe and successful control of vacuum arc remelting (VAR), a process used extensively throughout the specialty metals industry for the production of nickel base alloys and aerospace titanium alloys. Optimal estimation theory has been applied to the problem of estimating electrode gap and a filter has been developed based on a model of the gap dynamics. Taking into account the uncertainty in the process inputs and noise in the measured process variables, the filter provides corrected estimates of electrode gap that have error variances two-to-three orders of magnitude less than estimates based solely on measurements for the sample times of interest. This is demonstrated through simulations and confirmed by tests on the VAR furnace at Sandia National Laboratories. Furthermore, the estimates are inherently stable against common process disturbances that affect electrode gap measurement and melting rate. This is not only important for preventing (or minimizing) the formation of solidification defects during VAR of nickel base alloys, but of importance for high current processing of titanium alloys where loss of gap control can lead to a catastrophic, explosive failure of the process.

I. INTRODUCTION

Vacuum arc remelting (VAR) is a process used throughout the specialty metals industry for controlled casting of segregation sensitive and reactive metal alloys. Of particular importance in the former group are nickel base superalloys, whereas common reactive metal alloys include titanium and zirconium alloys. In this process, a cylindrically shaped, alloy electrode is loaded into the water-cooled, copper crucible of a VAR furnace, the furnace is evacuated, and a DC arc is struck between the electrode (cathode) and some start material (e.g. metal chips) at the bottom of the crucible (anode). The arc heats both the start material and the electrode tip, eventually melting both. As the electrode tip is melted away, molten metal drips off and an ingot forms in the copper crucible. Because the crucible diameter is typically 0.05-0.15 m larger than the electrode diameter, the electrode must be translated downward toward the anode pool to keep the mean distance between the electrode tip and pool surface constant; this mean distance is called the electrode gap (G). The objective of VAR is to produce an ingot of appropriate grain structure that is free of segregation, porosity, shrinkage cavities, or any other defects associated with uncontrolled solidification during casting. The VAR process is schematically depicted in Figure 1.

G is an extremely important control parameter for VAR.[1] If this variable becomes too large, the arc will search for a less resistive path to ground with the result that a greater percentage of arc energy will be collected by the crucible wall above the ingot pool surface. This gives rise to both a decrease in, and a redistribution of, the energy flux to the electrode tip and anode pool. If this condition persists, disruption of the

solidification process occurs and the probability of producing ingot defects increases. In severe cases, the arc may completely attach to the crucible and burn a hole in it, admitting cooling water into the melt. This is a major safety concern for high current (30-40 kA) VAR of reactive metals where such situations have caused furnace explosions and loss of life. On the other hand, if G is too small (<0.006 m, which is of the same order as the amplitude of the liquid motion on the pool and electrode tip surfaces), transient arc interruptions occur due to multiple, nearly simultaneous contacts between the electrode and ingot.[2] This leads to decreased melt rate, process instability, and disruption of the solidification process. Again, if this situation persists, ingot defects may be generated.

Successful VAR practice requires careful control of electrode gap. Because it cannot be measured directly by non-intrusive methods, a related process variable must be measured and used for this purpose. Most modern VAR control systems use either process voltage or drip-short frequency as a control variable for G.[3] The former is used in high current titanium and zirconium VAR while the latter is commonly used for VAR of nickel base alloys and steels. A typical way of controlling gap while melting at constant current is to adjust the electrode drive velocity (V) or position (X) so as to maintain the measured control variable at its setpoint. A simple proportional controller is often adequate for this purpose so long as the process is maintained in a region of control space where the control variable responds linearly to the control input.

A more intelligent method of control requires developing a measurement model for G as a function of related process variables, e.g. melting current, voltage and pressure.[4] V or X is then adjusted at appropriate time intervals to maintain the model-based measure of G at G^0, the setpoint. This method has the advantage of being tolerant of changes in

the system variables used in the measurement model so long as the process is held within the region of control space for which the model is valid. It has an additional advantage in that it constitutes an inherently linear means of control. For example, because G is a nonlinear function of drip-short frequency, a change in X does not produce a proportional change in drip-short frequency. Thus, except within a small range considered to be approximately linear, the proportional gain used in the controller will produce a control signal that is either too small or too large. This may cause the controller to become unstable. However, a change in X always produces a proportional change in G. Control based on estimates of G may be used to extend the range of control into regions of control space unavailable to simple voltage or drip-short controllers without special means being provided to deal with nonlinear responses.

There are some problems associated with simply estimating gap from voltage or drip-short measurements and using this information in a controller. First, these measurements tend to be very noisy and this requires that the data be averaged over a relatively long period (20-60 seconds) before being used as the basis for a control decision. Even so, it is difficult to accurately estimate G to better than a few millimeters under the best of conditions and this requires designing a relatively highly damped controller. Second, control based solely on measurement models assumes that a valid model is available for all conditions encountered during the process. If a disturbance occurs that invalidates the normal model, the controller must detect it and implement control based on a new model, valid for the disturbance condition, or apply a robust default control mode. Thus, effective control requires that process upsets be detectable

and that measurement models or appropriate default control methods are available for each upset condition.

The issue of measurement noise and its effect on controller response is very important. One method of dealing with this issue, recently patented by Hysinger et. al., is to incorporate a process observer into the control system.[5] In the sense of state space control theory, an observer is a dynamic system the state of which is defined by a set of variables that are the estimates of the state variables of the system to be controlled.[6] It is assumed that the state of the system is completely determined once the values of the state variables have been specified. For the specific case of electrode gap control during VAR, the observer must incorporate a dynamic model of the process that involves estimates of those state variables affecting electrode gap. The observer may be constructed in such a way as to output improved estimates of the state variables and measured outputs of the system. In fact, it was demonstrated in the 1960's that an optimum observer could be constructed, called a Kalman filter, that yields the best possible estimates of the state variables and measured outputs given the process variables, measurement and process noise characteristics, and assuming a linear state model.[7]

In this paper, Kalman filter technology is applied to the problem of estimating electrode gap during VAR. The filter development is discussed in Section II. In that section, a simple state-space model of the VAR process is presented. Section III describes simulations performed to evaluate the effectiveness of the filter in reducing the noise in electrode gap estimates. The performance of the filter during common process disturbances is also simulated. Though the main purpose of this paper is to focus on the filter design and development work, an example is provided of filter performance from a

test using the VAR furnace at the Liquid Metals Processing Laboratory at Sandia National Laboratories. The test work, including industrial tests, will be described in detail in a later publication. Finally, the performance of the filter is discussed in Section IV.

II. FILTER DEVELOPMENT

The electrode gap dynamics are described by the following equation:

$$\dot{G} = \dot{l}_{el} - \dot{h}_{ing} - V . \qquad [1]$$

This equation states that, over a very short time interval, the change in gap equals the change in electrode length (l_{el}) due to melting minus the change in ingot height (h_{ing}) due to mold filling and the distance the electrode was moved. The first term on the right can be found by assuming that liquid metal leaves the surface as soon as it forms and that the electrode tip surface is flat with an area given by εA_e where A_e is the room temperature cross-sectional area and ε accounts for the effects of thermal expansion. The resulting expression is

$$\dot{l}_{el} = \frac{R}{\rho_{liq} \varepsilon A_e} \qquad [2]$$

where R is the electrode melting rate and ρ_{liq} is the liquid metal alloy density.

The second term in Eq. [1] is directly related to the first since the ingot is formed from material melted off the electrode. The relationship is complicated by the fact that the ingot is being cooled and its density is a function of both ingot height and radial ingot position. In steady-state, it is assumed that the change in ingot height with time can be described by

$$\dot{h}_{ing} = \kappa \frac{A_e}{A_i} \dot{l}_{el} \qquad [3]$$

where k is a factor that corrects the room temperature electrode/ingot area ratio (often called the fill ratio) for thermal effects. This is born out in practice where it is found that, under steady-state melting conditions, a linear drive speed is required to achieve a constant electrode gap.

Substituting Eq.'s [2] and [3] into Eq. [1] gives the following expressions for the time dependent gap behavior:

$$\dot{G} = \frac{1}{\rho_l \varepsilon}\left(\frac{1}{A_e} - \frac{\kappa}{A_i}\right)R - V = \alpha R - V \qquad [4]$$

In practice, an average α for a particular process is estimated from melt data. Eq. [4] is integrated and solved for α. The resulting equation is then evaluated by supplying data for the initial and final gaps, the total mass melted and the total distance the electrode was moved during the melt.

Standard state-space methods were used to describe the VAR electrode gap dynamics. This technique assumes that the state of the process, or plant, is determined by specifying the values of the state variables. These variables, taken together, form the state vector, x, of the system. The state variables chosen to describe the VAR process for this work were electrode gap, electrode mass (M), electrode position, and electrode melting rate.

Besides those variables needed to characterize the system, others are required to drive or "force" the system to change state. These process inputs form the input vector, u. There is only one input for this application, namely electrode drive velocity.

Given the state and input vectors, the discrete time process can be described by a matrix equation of the form

$$x_{n+1}=Ax_n+Bu_n+Nw_n \qquad [5]$$

where A, B and N are the transition, input, and process noise matrices, respectively. N operates on w, a vector characterizing the uncertainty in the inputs that drive the plant as well as uncertainty in the plant itself. These terms constitute the process noise. It is assumed that each component of w can be represented in discrete time by a white sequence with zero-mean. In other words, the process noise is uncorrelated and unbiased. The subscripts in Eq. [5] refer to time-steps in the discrete time system. A, B and N are determined by considering the gap dynamics of the VAR process.

As seen above, changes in electrode gap are directly related to the relative velocities of the growing ingot and moving, melting electrode. Converting Eq. [4] to discrete time and accounting for process uncertainty, the electrode gap dynamics are described by

$$G_{n+1} = G_n + \alpha R_n T - V_n T - w_{X_n(V)} + R_0 T w_{\alpha_n} \qquad [6]$$

where T is the sample time, R_0 is the nominal melt rate, $w_{X_n(V)}$ quantifies the uncertainty in electrode position due to uncertainty in the electrode drive velocity, and w_{α_n} quantifies uncertainty in α. This uncertainty stems from surface variations in both the electrode and crucible, variation in the electrode cross-sectional area due to voids, and fluctuating temperature distributions in both the electrode and ingot.

Changes in electrode mass are directly related to melt rate by

$$M_{n+1} = M_n - R_n T . \qquad [7]$$

In words, the mass at t_{n+1} is the mass at t_n less what melted off in the time interval.

Position changes are tied directly to velocity according to

$$X_{n+1} = X_n + V_n T + w_{X_n(V)} . \qquad [8]$$

The position at t_{n+1} is just the position at t_n plus the distance moved in the last time step corrected for the uncertainty in the electrode drive velocity.

Finally, this formulation assumes that the melt rate is a random variable with no driving term so that the dynamics are simply described by

$$R_{n+1} = R_n + w_{R_n} \qquad [9]$$

where w_{R_n} quantifies the uncertainty in the melt rate. Note that Eq. [9] does not guarantee that the melt rate will remain indefinitely at its initial value. Indeed, over a time period consisting of many time steps it will randomly walk away from that value, the maximum step size of the walk being determined by the uncertainty. In practice, the plant behavior differs from this because one attempts to drive the melt rate with melting current. Insofar as the development of the filter is concerned, this is irrelevant so long as one has correctly accounted for the process and measurement noise sources.[8]

The development has assumed a straight electrode and crucible: A_e and A_i are not functions of time. However, it is often the case that melting is performed with both tapered electrode and crucible for the simple reason that a tapered casting is easier to remove from the mold. Because of this, it is not uncommon for α to vary linearly by 10-20% over the duration of a VAR melt. One may easily account for this non-random error by modeling the time-dependent behavior of α, an exercise that adds complication to the filter development but nothing conceptually to the way it works and performs. For this reason, the more complicated formulation is not given here. However, a simple method of including this feature in the model is to linearize Eq. [4] about the nominal values (α_0,R_0,V_0), and then add a new state variable $\Delta\alpha=\alpha-\alpha 0$ where α is now a function of the amount of material melted.

Making appropriate substitutions, Eq. [5] can be written as

$$\begin{bmatrix} G_{n+1} \\ M_{n+1} \\ X_{n+1} \\ R_{n+1} \end{bmatrix} = A \begin{bmatrix} G_n \\ M_n \\ X_n \\ R_n \end{bmatrix} + B[V_n] + N \begin{bmatrix} w_{X_n(V)} \\ w_{\alpha_n} \\ w_{R_n} \end{bmatrix}. \qquad [10]$$

which relates the electrode gap, mass, position and melt rate at t_{n+1} to their values at t_n given both deterministic and random inputs. A, B and N can now be derived from inspection of Eq.'s [6]-[10]. They are

$$A = \begin{bmatrix} 1 & 0 & 0 & \alpha T \\ 0 & 1 & 0 & -T \\ 0 & 0 & 1 & 0 \\ 0 & 0 & 0 & 1 \end{bmatrix} \qquad [11]$$

$$B = \begin{bmatrix} -T \\ 0 \\ T \\ 0 \end{bmatrix} \qquad [12]$$

and

$$N = \begin{bmatrix} -1 & R_0 T & 0 \\ 0 & 0 & 0 \\ 1 & 0 & 0 \\ 0 & 0 & 1 \end{bmatrix}. \qquad [13]$$

Besides state variables and inputs, the system is also characterized by outputs, some, or all, of which can be measured. The outputs for this system are taken to be electrode gap, mass and position. The output equation is then given by

$$\begin{bmatrix} G_n \\ M_n \\ X_n \end{bmatrix} = C \begin{bmatrix} G_n \\ M_n \\ X_n \\ R_n \end{bmatrix}. \qquad [14]$$

Again by inspection, it is seen the C must be given by

$$C = \begin{bmatrix} 1 & 0 & 0 & 0 \\ 0 & 1 & 0 & 0 \\ 0 & 0 & 1 & 0 \end{bmatrix}. \qquad [15]$$

Assuming that all outputs can be measured, the measurements at t_n are modeled by

$$z_n = C \begin{bmatrix} G_n \\ M_n \\ X_n \\ R_n \end{bmatrix} + \begin{bmatrix} v_{G_n} \\ v_{M_n} \\ v_{X_n} \end{bmatrix} \qquad [16]$$

where the elements of the column vector, v_n, characterize the measurement noise (assumed white with zero mean) present in the gap, mass and position measurements.

Given the process and measurement models embodied in Eq.'s [6]–[16], a Kalman filter (or optimal state observer) can be constructed using known methods the details of

which are presented in standard texts on modern control system design.[9] The equation for the filter in discrete time is

$$\hat{x}_{n+1}=A\hat{x}_n+Bu_n+M_K\left(z_n-C\hat{x}_n\right) \qquad [17]$$

where A, B and C are as defined above for the plant, and a "hat" over a variable denotes an estimate. $\hat{x}_{n+1}$ is the predicted system state at t_{n+1} estimated from measurements and the estimated state at t_n. The Kalman matrix, M_K, is chosen so as to minimize the error covariance of the estimated variables relative to their true values and can be derived from the steady-state process and measurement noise covariances. Each column of M_K corresponds to one of the measured system outputs, while each row is associated with a state variable. In the present application, M_K is a 4x3 matrix. Off-diagonal elements arise because of couplings between the variables. For example, $\hat{G}$ is related to the measured values of all three outputs since $w_{X_n(V)}$ is a position term and melt rate is directly related to electrode mass (Eq. [6]). Therefore, the first row of M_K contains all non-zero values. On the other hand, there is no measurement for α and, thus, no corresponding element in M_K. The difference term in Eq. [17], called the innovation, goes to zero only in the case where the measurements are noise free and match perfectly the model predictions. In this situation, the future state is perfectly predicted from the present state by the system model, and all estimated values exactly equal the actual values. This situation never holds in practice.

The Kalman filter produces estimates of the future state and current outputs. These estimates are tied to process and measurement noise through a model of the system

according to an optimal weighting scheme. If the process inputs and parameters are known with a high degree of precision relative to the measured outputs, the estimates will not be greatly influenced by the measurements, i.e. the filter "knows" that the measurements cannot be trusted. In this case, the elements of M_K will be very small and the estimator will be model based. The filter simply takes advantage of the fact that the state of the system is nearly completely determined by the physical constraints placed on it by the inputs and process variables coupled with knowledge of the previous state. On the other hand, if relatively exact measurements are available, the estimator will weigh them more heavily than the process model and the filter will be measurement based. Obviously, if all the outputs can be measured exactly, they do not need to be estimated.

III. SIMULATED FILTER PERFORMANCE

A block diagram of the VAR process model coupled to the Kalman filter in a feedback controller system is shown in Figure 2. A computer program was written using the Matlab™ programming language (The Math Works, Inc., Natick, MA) for the purpose of evaluating the improvement in the Kalman estimated outputs relative to the measured values. The simulations assume a 0.432 m (17 in.) diameter electrode being melted into 0.508 m (20 inch) diameter ingot at a nominal melt rate of 0.060 kg/s (476 lb/hr) and electrode drive speed of ~1.8×10^{-5} m/s (2.6 in./hr). These parameters are typical for VAR of Alloy 718. α is taken to be 2.94×10^{-4} m/kg based on experience melting this type and size material at this melt rate. This number is about 9% larger than

what would be obtained by simply setting $\varepsilon=\kappa=1$ in the expression for α. In the simulations, a sample time of 4 seconds was used.

Suppose, first, that the process is relatively noise free. The random sequences characterizing the process and measurement noise terms are each characterized by a standard deviation and variance. For the base simulations, $\sigma_{X(V)}$ was set to $2.0\text{x}10^{-6}$ m corresponding to an uncertainty in V of $5.0\text{x}10^{-7}$ m/s, and σ_R was set at $1.0\text{x}10^{-4}$ kg/s. σ_α was estimated to be $1.3\text{x}10^{-5}$ m/kg, or about 5% of the nominal value, by assuming that the electrode and crucible radii vary by only ±0.001 m over the duration of the melt, that the liquid density is known to ±100 kg/m^3, and that the other parameters are constant. The measurement noise (standard deviation) terms were set to $5\text{x}10^{-3}$ m, 1 kg and 10^{-3} m for v_G, v_M and v_X, respectively. These are believed to be typical of the measurement capabilities available on many VAR furnaces in industry.

Figure 3 shows a plot of G and $\hat{G}$ (its filtered value) resulting from a 5000 s simulation for an open-loop system. V was set to $1.755\text{x}10^{-5}$ m/s in this simulation. The figure demonstrates that $\hat{G}$ tracks the "true" gap very well. The drift in the gap from the nominal value of 0.01 m is due to the uncertainties in the system. Because the random errors in the system, the difference between the gap and its nominal value follows a random walk trajectory.

$\hat{G}$ is shown in Figure 4 plotted with the simulated measured electrode gap. The noise reduction achieved through Kalman filtering is readily apparent. This effect is seen in Table 1, Case 1, where error variances are tabulated for both the measured (upper numbers) and estimated (lower numbers) outputs of the simulation in the last three columns. Note that the variances in the simulated measurements always approximately

equal the squares of the specified measurement noise terms, as required. Also note that the error variance in $\hat{G}$ may vary by as much as a factor of two from simulation to simulation whereas the error variances for the other estimates are more stable.

Table 1. Open loop simulation results of the estimator performance.

Case No.	σ_G, σ_M, σ_X $\sigma_{X(V)}$, σ_R, σ_α	$Var.(\tilde{G}-G)$ $Var.(\hat{G}-G)$	$Var.(\tilde{M}-M)$ $Var.(\hat{M}-M)$	$Var.(\tilde{X}-X)$ $Var.(\hat{X}-X)$
1	$5.0\text{x}10^{-3}$, 1.0, $1.0\text{x}10^{-3}$ $2.0\text{x}10^{-6}$, $1.0\text{x}10^{-4}$, $1.3\text{x}10^{-5}$	$2.5\text{x}10^{-5}$ $1.3\text{x}10^{-8}$	0.99 $2.5\text{x}10^{-2}$	$9.7\text{x}10^{-7}$ $2.3\text{x}10^{-9}$
2	$5.0\text{x}10^{-3}$, 1.0, $1.0\text{x}10^{-3}$ $\underline{4.0\text{x}10^{-5}}$, $1.0\text{x}10^{-4}$, $1.3\text{x}10^{-5}$	$2.4\text{x}10^{-5}$ $5.7\text{x}10^{-8}$	1.0 $2.9\text{x}10^{-2}$	$9.9\text{x}10^{-7}$ $3.9\text{x}10^{-8}$
3	$5.0\text{x}10^{-3}$, 5.0, $1.0\text{x}10^{-3}$ $2.0\text{x}10^{-6}$, $\underline{1.0\text{x}10^{-3}}$, $1.3\text{x}10^{-5}$	$2.5\text{x}10^{-5}$ $2.4\text{x}10^{-8}$	0.98 $8.5\text{x}10^{-2}$	$1.0\text{x}10^{-7}$ $2.0\text{x}10^{-9}$
4	$5.0\text{x}10^{-3}$, 5.0, $1.0\text{x}10^{-3}$ $2.0\text{x}10^{-6}$, $1.0\text{x}10^{-4}$, $\underline{5.4\text{x}10^{-5}}$	$2.5\text{x}10^{-5}$ $7.3\text{x}10^{-8}$	0.99 $2.8\text{x}10^{-2}$	$1.0\text{x}10^{-6}$ $2.1\text{x}10^{-9}$
5	$\underline{5.0\text{x}10^{-4}}$, 1.0, $1.0\text{x}10^{-3}$ $2.0\text{x}10^{-6}$, $1.0\text{x}10^{-4}$, $1.3\text{x}10^{-5}$	$2.5\text{x}10^{-7}$ $3.2\text{x}10^{-9}$	1.0 $2.5\text{x}10^{-2}$	$9.9\text{x}10^{-7}$ $1.7\text{x}10^{-9}$
6	$5.0\text{x}10^{-3}$, $\underline{10.0}$, $1.0\text{x}10^{-3}$ $2.0\text{x}10^{-6}$, $1.0\text{x}10^{-4}$, $1.3\text{x}10^{-5}$	$2.5\text{x}10^{-5}$ $7.4\text{x}10^{-8}$	99 0.78	$9.9\text{x}10^{-7}$ $2.0\text{x}10^{-9}$
7	$5.0\text{x}10^{-3}$, 1.0, $\underline{1.0\text{x}10^{-4}}$ $2.0\text{x}10^{-6}$, $1.0\text{x}10^{-4}$, $1.3\text{x}10^{-5}$	$2.4\text{x}10^{-5}$ $1.7\text{x}10^{-8}$	1.0 $2.7\text{x}10^{-2}$	$9.9\text{x}10^{-9}$ $2.1\text{x}10^{-10}$

The large noise reductions in the estimated outputs are due to the small process uncertainties relative to the measurement errors. Physically, if the drive speed, melt rate and furnace dimensions are accurately known with a high degree of precision, the plant outputs are determined to a corresponding precision. However, it may be the case that the process uncertainties are not so precise. How are the various estimates affected by increasing the process errors?

Typically, modern electrode drive controls are rather advanced and drive speed is accurately controlled to a relatively high degree of precision. However, if instead of controlling the speed to $\pm 5 \times 10^{-7}$ m/s, one controls to within $\pm 10^{-5}$ m/s, one obtains the results shown in Table 1, Case 2. The error variances in the estimates of G and X are seen to increase while that of M remains unchanged. This is to be expected since this latter variable is independent of ram velocity and position (Eq. [7]). It should be noted from the table that, even with relatively poor ram control, the uncertainty in $\hat{G}$ is still much smaller than that observed in the measurement.

Next consider the uncertainty in the melt rate. It has been assumed that this uncertainty is $\pm 10^{-4}$ kg/s at steady-state current in the absence of any process disturbance. In effect, this says that the melt rate will not vary by more than this in a single time step. Suppose, now, that the uncertainty is an order-of-magnitude larger, namely $\pm 10^{-3}$ kg/s. As may be see from Table 1, Case 3, increasing the uncertainty in the melt rate produces a concomitant increase in the error variance of $\hat{M}$, little if any change in that of $\hat{G}$, and has no affect on that of $\hat{X}$. In a like manner, decreasing the uncertainty in the melt rate decreases the error covariance of $\hat{M}$ but has no effect on that of the other variables. These changes do affect the open-loop performance of the system as would be expected.

However, because the error in the gap estimate remains relatively unchanged, they do not significantly affect the closed-loop performance of the system for gap control.

Finally, $\hat{G}$ is expected to be sensitive to uncertainty in the process parameter α. Suppose α has an uncertainty of 20% instead of 5%. The simulation results for this case are shown in Table 1, Case 4. It is apparent that the gap estimate has been degraded a small amount but that it is still much better than the corresponding measurement. The error variances of the other estimates are unaffected as one would expect from Eq.'s [7] and [8]. It should be noted that the Kalman filter corresponding to Case 4, when used with a standard tapered electrode and crucible combination, yields a maximum bias in the gap estimate of ~0.001 m.

One can also use the estimator simulation to investigate the effects of changing the resolutions of the measurements. It turns out that the error in $\hat{G}$ increases by a factor of four or five with an order of magnitude increase in electrode gap measurement noise. However, further increases have little effect. The effect of increasing the measurement resolution to ±0.0005 m is shown in Table 1, Case 5. Further increases in resolution result in concomitant decreases in estimation error illustrating the trivial point that one does not need to estimate variables that can be measured accurately with high precision. At a measurement error of $\pm 5 \times 10^{-6}$ m, the error variance of the measurement equals that of the estimate.

Table 1, Case 6 shows an increase in uncertainty in $\hat{G}$ when increasing the mass measurement error from ±1 to ±10 kg. However, increases beyond ±20 kg have no significant effect on the estimation error for G. It was also observed that increasing the

mass measurement resolution had no significant effect on the uncertainty in $\hat{G}$ though it does, of course, affect the error in $\hat{M}$.

Finally, the variance of $\hat{G}$ is not particularly sensitive to changes in the measurement error of X under these process conditions. Table 1, Case 7 shows the results of a ten-fold increase in position measurement resolution. It is seen that the change is only reflected in the error variance of $\hat{X}$.

The simulation results show that significant noise reduction can be achieved in electrode gap estimates by using Kalman filtering. It is of interest to determine how the estimator responds to common disturbances. A disturbance (upset) is defined as any change in the system state that cannot be controlled by varying the inputs. Three common system disturbances will be considered here: 1) variation in melt rate due to a cracked electrode; 2) a "glow" condition wherein both melt rate and measured electrode gap are affected; and 3) a gap measurement upset wherein the measured gap is consistently smaller than the true gap. One anticipates that, given the definition of a disturbance, the performance of the estimator will be adversely affected. To carry out this study, a simulator program was written corresponding to the feedback system in Figure 2.

A common form of melt rate disturbance is caused by a transverse crack in the electrode. As the melt zone approaches the crack, melt rate increases because the crack impedes heat conduction along the electrode length. When the zone burns through the crack and encounters the relatively cool material on the other side, melt rate suddenly drops. This type of disturbance was simulated by applying a linear ramp to the melt rate variable of the system model so that melt rate increased from nominal to nominal plus 20% over a period of 5000 seconds. At the end of the ramp, melt rate was instantaneously

dropped to nominal minus 20% and ramped back to nominal over 5000 seconds. Because the velocity input cannot control the formation of a crack, it is clear that this condition constitutes a disturbance to this system. How does the filter perform under these circumstances?

Figure 5 shows the actual and estimated values of electrode gap during the disturbance for an open-loop (constant drive speed) configuration using the same Kalman gains used for the simulation results shown in Table 1, Case 1. It is clear from the figure that the estimator is, for the most part, able to track the disturbance. The reason for this is clearly seen in Figure 6 which shows a plot of the estimated melt rate state variable. The filter uses the available measurement information to infer melt rate estimates consistent with the data. It is able to track the upset as long as σ_R is not small relative to the ramp rate. In other words, the estimate will lag the disturbance only if the change in melt rate due to the disturbance is much larger than the amount the model allows the melt rate to change in a single time step. For example, decreasing σ_R by an order-of-magnitude causes the estimate to seriously lag the disturbance. If the simulation is run with feedback, the results shown in Figure 7 are obtained. It is evident from the figure that the estimated output does not perfectly respond to the melt rate disturbance at the instantaneous step as one might expect. However, the gap only varies by about 0.001 m at this point.

Suppose now that one encounters a "glow" condition in the furnace.[10] This condition occurs when the arc transfers, either partially or completely, from the electrode tip onto the relatively cold electrode lateral surface. It is most often caused by oxide contamination of the electrode or an air leak. Besides the characteristic "glow" in the

furnace annulus, the condition is typically characterized by a decrease of a few volts in arc voltage accompanied by a significant increase in furnace head pressure. During a glow, drip-shorts and melting are commonly observed to cease. The condition may last only a few seconds, or it may persist for several minutes and occur at regular intervals throughout a melt. Obviously, this condition comprises a system disturbance: ram velocity cannot be used to turn the glow on or off.

Glow was simulated by allowing the melt rate to suddenly drop to zero for sixty seconds. Because drip-shorts disappear during the glow and arc voltage decreases, the measurement based electrode gap estimate suddenly becomes very large during this condition. It is assumed that logic is built into the controller that does not allow the measurement based estimate to exceed the range of the validity of the measurement technique. For drip-short based measurements, the upper end of this range is about 0.025 m beyond which the response becomes very flat. Therefore, in the simulation, when the melt rate perturbation goes to zero, the gap perturbation is set to 0.025 m for the same time period.

Figure 8 shows the results of the open loop (constant drive speed) response to the simulated glow with the original Kalman gains. The sudden decrease in estimated gap is related to the sudden decrease in melt rate. Despite the increase in the measured value, the estimator weighs the sudden drop in melt rate more heavily and estimates that the gap is closing at the open loop drive speed. The closed loop controller results are shown in Figure 9. The sharp decrease in gap of about 0.001 m occurs because the estimated melt rate lags the true melt rate by a small amount as seen in Figure 8. This is supported by the

observation that increasing the melt rate uncertainty serves to make the "spike" in Figure 9 shallower and narrower.

The third disturbance to be simulated is one in which the measured electrode gap is consistently small. This disturbance was simulated by introducing a -0.005 m bias into the electrode gap measurement. The open loop response to the bias is shown in Figure 10. The bias was applied at t=5000 seconds and ended at t=10,000 s. It is readily apparent from the figure that the estimator responds to the incorrect measurement and requires >10,000 s to recover. The closed loop system gives the result shown in Figure 11. It is seen from the figure that the discrepancy between the estimated and true gap grows to nearly 0.003 m over the 5000 s interval.

The simulations were performed for hypothetical situations considered to be typical of actual VAR processes. As mentioned in the Introduction, the primary focus of this paper is on the filter development and simulation results. However, it is appropriate to show some sample data to verify that the predicted improvements in noise are realized in actual practice.

The data shown in Figure 12 were acquired during VAR of 0.203 m diameter Alloy 718 electrode into 0.254 m diameter ingot on the VAR furnace at Sandia National Laboratories. Neither the electrode nor the crucible were tapered. Because there is no mass transducer (load cell) on this furnace, the measurement uncertainty is infinite for electrode mass. Melt rate during the interval shown was estimated to be 0.040±0.002 kg/s and the drive speed noise was similar to that used in Table 1, Case 1. A high resolution encoder is mounted on the furnace so that the resolution in X was 10^{-5} m. The noise variance in the drip-short based measurement of G was 2.6×10^{-5} m^2. In comparison, the

variance in the Kalman filter estimate of G was 5.1×10^{-9} m^2 giving a signal to noise improvement of about 70. Drive speed control decisions were made every two seconds based on the filtered estimates. The controller was stable at very tight gaps (0.006 m). Intrusive gap measurements accomplished by driving the ram down until a dead short was achieved demonstrated that the controller was accurate to within the intrusive measurement error (±0.001 m).

IV. DISCUSSION

Optimal estimation techniques were originally developed for application to systems where measurements of key process variables were either very noisy or unavailable. It is natural to apply this technology to controlling the electrode gap in the VAR process where one encounters noisy measurements that are often spoiled by common process disturbances.

Kalman filtering achieves dramatic noise reduction in the estimate of the electrode gap relative to voltage or drip-short based measurements on the same time scale. After only a few seconds of data acquisition, it is to be expected that drip-short or voltage based estimates of electrode gap will be highly inaccurate due to measurement noise. However, given the process inputs and noise, and the last state estimate, one can determine, based on physics alone, how much the gap could possibly have changed during the last time step. It is this physics-based limitation that the filter imposes on the gap measurement, and this is the reason for the large noise reduction in the estimate.

Gap estimation was found to be sensitive to either increases or decreases in the gap measurement error indicating that the estimator, as defined, is neither model- nor measurement-based. However, estimates are insensitive to measurement error once it has been increased beyond about ±0.1 m, indicating that the estimator is model-based under these measurement conditions. In other words, if one cannot measure gap to better than ±0.1 m under these process conditions, the measurement is irrelevant to gap estimation. On the other hand, the estimator is completely measurement-based with respect to gap measurement at a measurement resolution of $\pm 5 \times 10^{-6}$ m. At this resolution, the estimator becomes superfluous.

Besides electrode gap estimates, the Kalman filter supplies estimates of melt rate. This variable is very difficult to measure from load cell data being extremely sensitive to noise in the transducer because it involves taking a derivative of the transducer output. Because of this, melt rate data are often averaged for as long as twenty minutes to obtain a moderately noise-free measurement. Such highly damped measurements are useless for gap control. However, the Kalman filter produces estimates of melt rate on the same time scale used to make control decisions. These estimates are consistent with the system model, measured variables, and noise parameters that characterize the process. The melt rate noise parameter, w_R, can be tuned to make the filter either more or less responsive to melt rate excursions. This provides a means of tracking melt rate deviations that would go undetected by highly damped measurement systems.

The simulation results show that accurate mass measurements (±1 kg) are beneficial for electrode gap estimation. Improvements beyond this have little effect. Increasing the measurement error adversely affects the gap estimate up to about ±20 kg. Under the

process conditions investigated, one might as well have no mass measurement at all if the error is increased beyond this value. Thus, with respect to electrode mass measurement, the estimator is model-based beyond a measurement error of about ±20 kg and measurement-based at measurement errors less than ±1 kg.

The results indicate that gap estimation is not improved significantly by improving the resolution of the position measurement under the simulation conditions investigated. One must resist concluding from this that exact position measurements are of little intrinsic value to gap estimation. This depends on the uncertainties characterizing the system. For example, if one has poor ram control (Table 1, Case 2), the error covariance in $\hat{G}$ may be significantly reduced by increasing the position measurement resolution to $\pm 10^{-4}$ m, a figure that is easily achievable with commercially available encoder systems. In general, complete system characterization is required before one can decide how to improve the estimation of important process variables.

The performance of the Kalman estimator was investigated to determine how it performed during common process disturbances. A control method that falls apart during minor process upsets is of little value without developing techniques of disturbance detection and management. It was discovered that the filter responds very predictably to the upsets investigated and that it behaved robustly during rather severe melt rate perturbations and extended glows.

Glows are relatively easy to detect in practice and logic can be built into the controller to more effectively deal with this condition if the kind of response shown in Figure 9 is deemed inadequate. For example, the commanded ram velocity could be set to zero during a glow and the gap estimate held at its pre-glow value. Alternatively, one

could gain schedule, loading in a Kalman gain matrix during the disturbance that weighted the mass measurement more and the gap measurement less. This would have the effect of stopping the ram until the glow condition ended because the measured mass would not change significantly (i.e. relative to the measurement uncertainty) during the disturbance.

The third disturbance to be simulated, the biased gap measurement, is one that occasionally occurs during high current titanium melting. It sometimes happens that the arc attaches to the crucible wall for a time, or, in the case of an off-center electrode, burns on the side of the electrode closest to the crucible wall where the point of minimum gap exists. An axial magnetic field is applied to facilitate arc rotation and prevent this from occurring, but in some cases the field is not strong enough to give rise to rotation. Under these conditions, the arc voltage is smaller than normal causing the measured electrode gap to be smaller than the true gap between the electrode tip and ingot pool surface. In this situation, moving the electrode has little effect on the measurement because the distance between the crucible wall and electrode tip remains relatively constant. A conventional controller responds by slowing the ram velocity, or even backing the ram out, which causes the arc to be more firmly attached to the crucible wall thereby causing the actual electrode gap to become very large over time. At any time during such an upset, if the arc becomes concentrated at a location on the crucible, it may burn through, causing a water leak into the molten titanium. At the very least, this ruins a crucible. However, it may also cause an explosion that destroys the furnace.

As demonstrated above, the optimal estimator explored in this simulation study can be configured to improve the response to this type of disturbance. The reason behind this

is that the estimator relies on an estimate of the electrode gap that is based on a process model as well as measured values. Thus, the response to the upset is damped by a factor that depends on how much the estimator weighs the gap measurement relative to the model-based estimate and other measurements. This is why the long-time response to the disturbance shown in Figure 11 is so small—the model, mass and position measurements, which are all correct to within their respective specified uncertainties, partially counteract the effects of the anomalous gap measurement. As a result, the controller does not react like a simple, measurement-based, proportional controller by pulling the electrode up or slowing the drive speed excessively. The electrode tip is kept relatively close to the molten metal pool surface minimizing the probability of a severe arc constriction onto the crucible wall.

At this level of process control, there is no complete solution to the upset problem. The response of the estimator will be compromised whenever process conditions are such that incorrect values are input to the filter. The next level involves characterizing the possible disturbance states and including disturbance state variables into the Kalman estimator. These types of controllers are presently under development at Sandia National Laboratories for application to VAR of U-6Nb alloy as well as for commercial alloys of interest to the SMPC.

V. CONCLUSIONS

The following conclusions can be made from this work:

1. Kalman filtering provides a potentially superior means of estimating electrode gap for VAR process control. The estimates are significantly less noisy and provide the basis for improving both the stability and response of the control system. Under the process conditions investigated, the measurement error in the electrode gap must be improved by three orders-of-magnitude to yield gap estimates equal to those of the estimator.

2. The Kalman filter development described here provides a means of estimating electrode melting rate that is not dependent on differentiating the load cell output. Hence, the estimates are not heavily damped and are useful for control purposes.

3. The error variance of the gap estimate could be affected by either increasing or decreasing the gap measurement uncertainty indicating that, under the process conditions of interest, the estimator was neither model-based nor measurement-based. Increasing the measurement error beyond ±0.1 m is equivalent to having no gap measurement at all.

4. An accurate electrode mass measurement is beneficial for electrode gap control up to an accuracy of ±1 kg under the process conditions investigated. Increasing the mass measurement error to ±20 kg is tantamount to having no mass data at all.

5. Increasing or decreasing the position measurement error has little effect unless one has poor ram control. With poor ram control, accurate, precise position measurement is beneficial.

6. The Kalman estimator was shown to be relatively robust with respect to common process disturbances. The three studied were 1) a melt rate disturbance due to a cracked electrode, 2) a glow disturbance associated with oxide contaminated melting or furnace air leaks, and 3) a gap measurement disturbance such as occurs during high current titanium melting when the electrode is not properly centered.

ACKNOWLEDGEMENTS

A portion of this work was supported by the United States Department of Energy under Contract DE-AC04-94AL85000. Sandia is a multiprogram laboratory operated by Sandia Corporation, a Lockheed Martin Company, for the United States Department of Energy. Additional support was supplied by the Specialty Metals Processing Consortium.

1. D. K. Melgaard, R. L. Williamson and J. J. Beaman: JOM, 1998, vol. 50(3), pp. 13-17.

2. R. L. Williamson and F. J. Zanner: *Proc. Vacuum Metallurgy Conf.*, N. Bhat, E. W. Bloore and D. R. Malley, editors, Iron and Steel Society, Warrendale, PA, 1992, pp. 87-91.

3. Drip-shorts are momentary arc interruptions due to metal drips bridging the electrode gap and contacting the ingot pool surface. See F. J. Zanner: *Metall. Trans. B*, 1979, 10B, pp. 133-42 for a detailed description of drip-short signatures, and reference [1] for a review of the various methods of control using process voltage and drip-shorts.

4. F. J. Zanner: *Metall. Trans. B*, 1981, 12B, pp. 721-8.

5. C. L. Hysinger, J. J. Beaman, D. K. Melgaard and R. L. Williamson: U. S. Patent #5,930,284, July 27, 1999. Also, see C. L. Hysinger, J. J. Beaman, R. L. Williamson and D. K. Melgaard: *Proc. of the 1999 International Symposium on Liquid Metal Processing and Casting*, American Vacuum Society, Santa Fe, New Mexico, 1999, pp. 145-55.

6. B. Friedland, *Control System Design, An Introduction to State Space Methods*, McGraw-Hill, Inc., New York, NY, 1986, p. 259.

7. See B. Friedland, Chapter 11, and references cited therein.

8. Though this paper is focused on electrode gap dynamics and control, it is possible to generalize the treatment to the dynamics of the VAR process as a whole, in which case it is essential to include the melt rate response to melting current.

9. See, for example, reference [5]. Also, *Applied Optimal Estimation*, A. Gelb, ed., M.I.T. Press, Cambridge, MA, 1994.

10. F.J. Zanner, L.A. Bertram, and R.L. Williamson: *Proc. Vacuum Metallurgy Conf.*, L.W. Lherbier and G.K. Bhat, eds., Iron and Steel Society, Pittsburgh, PA, 1986, pp. 49-54; R.L. Williamson, R. Harrison, R. Thompson and F.J. Zanner: *Proc. 11th International Conf. On Vacuum Metallurgy*, Antibes, France, May 11-14, 1992, pp. 128-30.

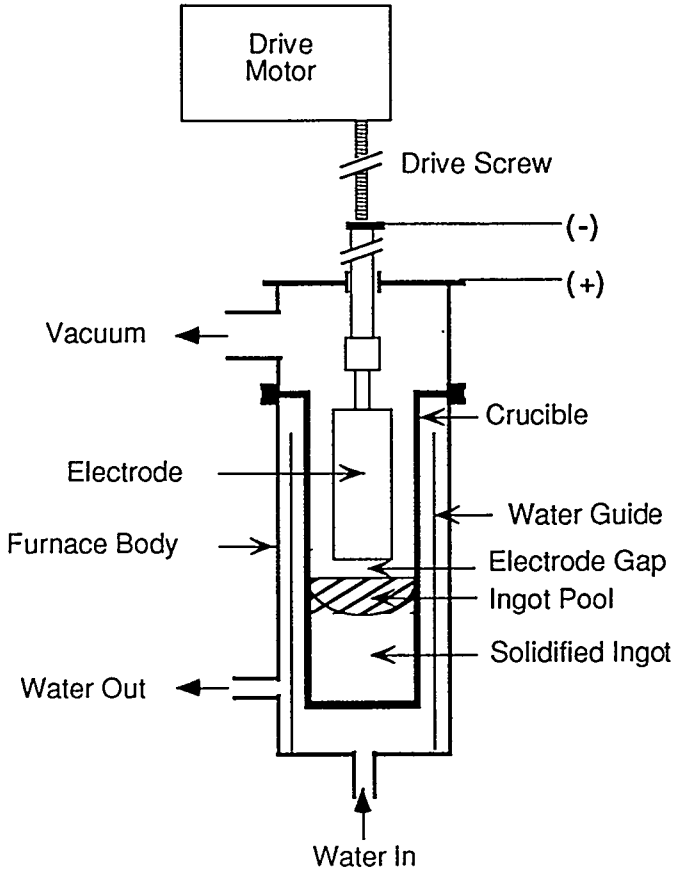

Figure 1. Schematic diagram of the VAR process.

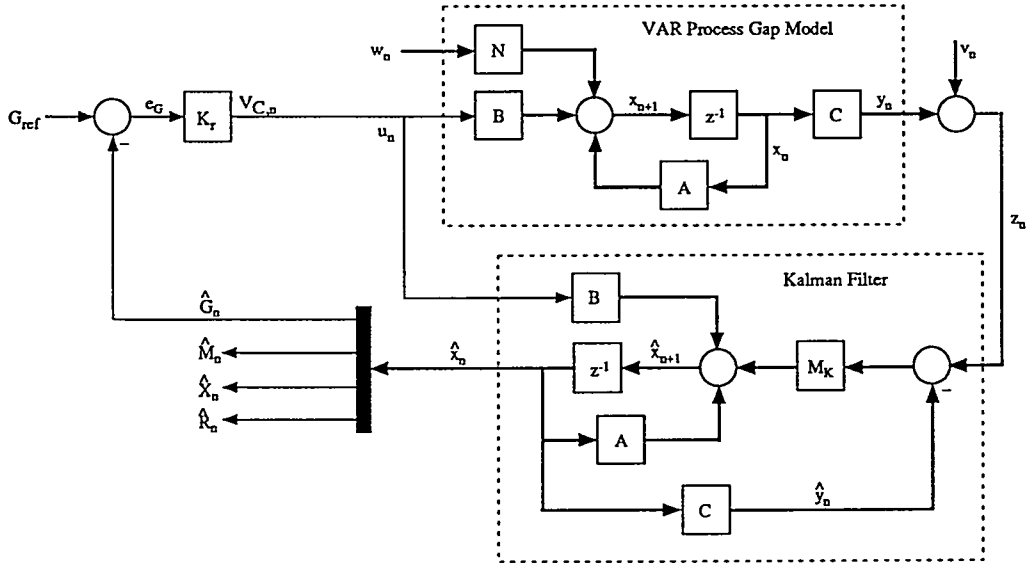

Figure 2. Feedback gap control incorporating a Kalman filter to estimate the system state (G, M, X, R) from measurement data. The heavier lines represent vectors.

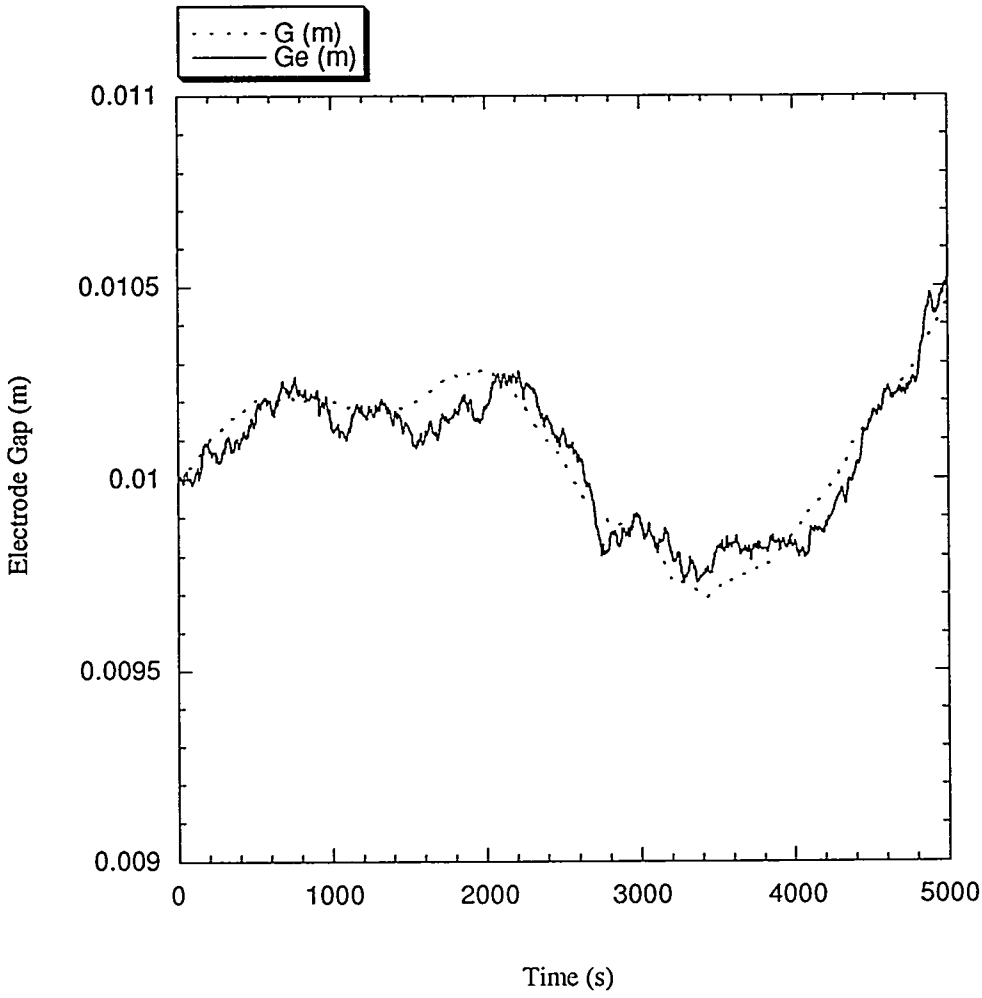

Figure 3. Open-loop simulated electrode gap estimate (Ge) and "true" electrode gap (G) plotted for 5000 s.

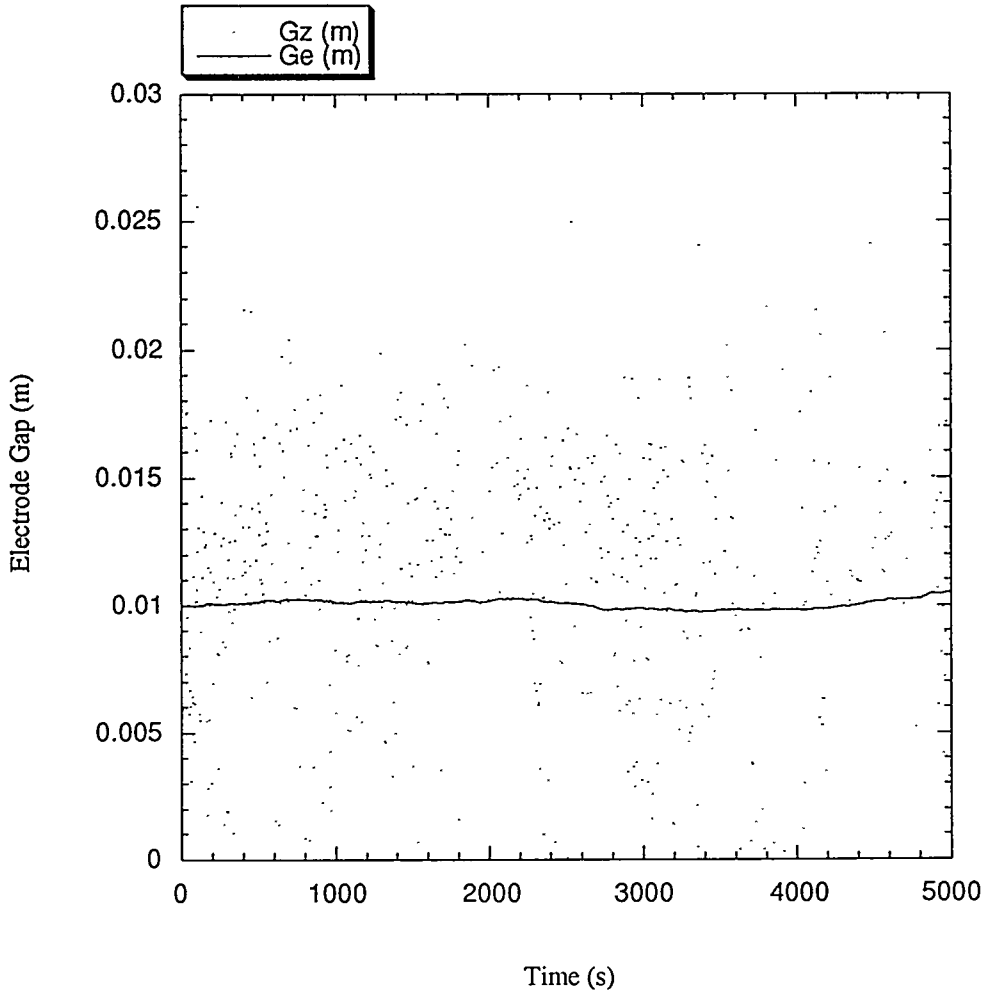

Figure 4. Open-loop simulated electrode gap estimate (Ge) plotted with the "measured" value (Gz).

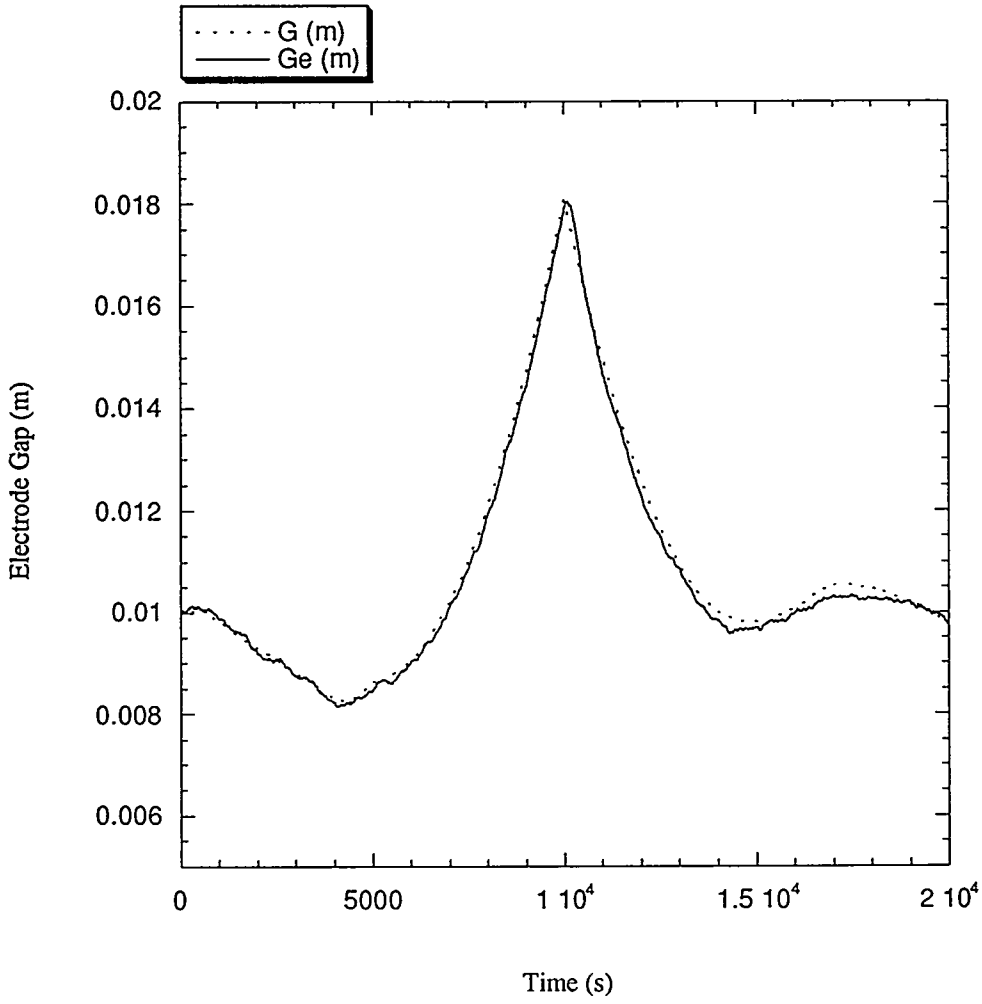

Figure 5. Plot showing the open-loop estimator tracking a simulated melt rate event where the melt rate linearly increases to 20% above nominal between t=5000 and t=10,000 seconds, suddenly drops to 20% below nominal at t=10,000 seconds, and then linearly returns to nominal between t=10,000 and t=15,000 seconds.

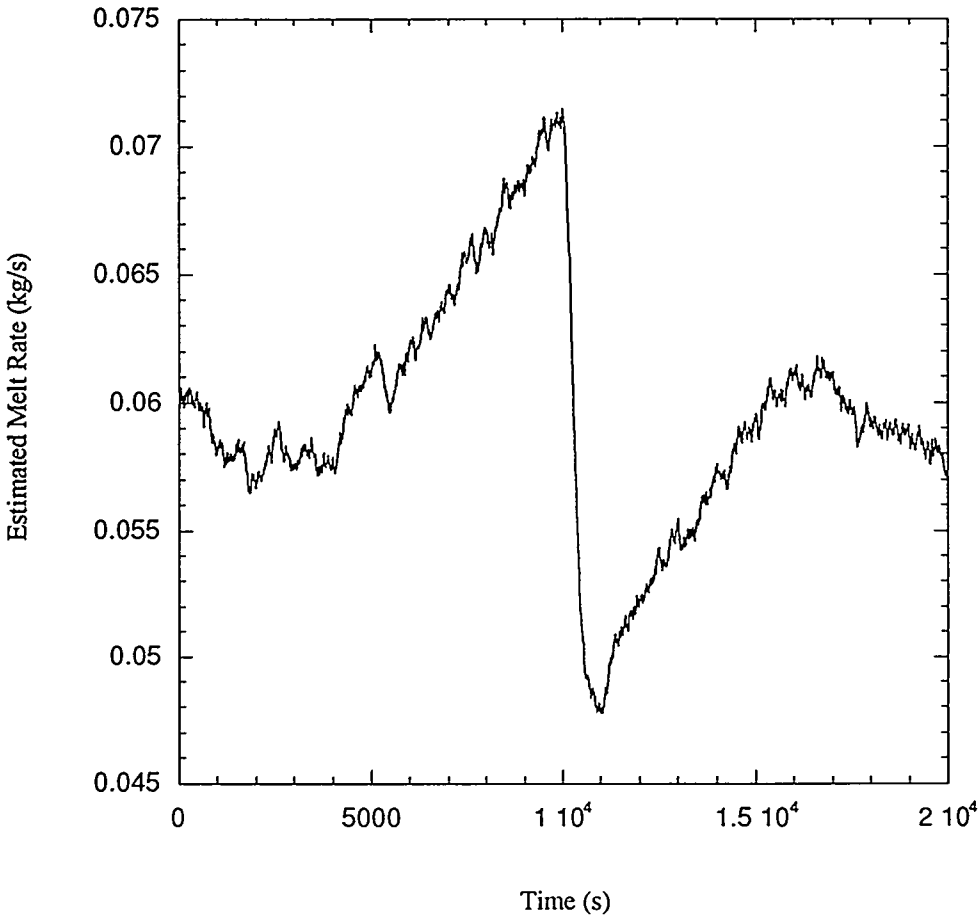

Figure 6. Plot showing the Kalman filter's estimate of melt rate during the melt rate disturbance.

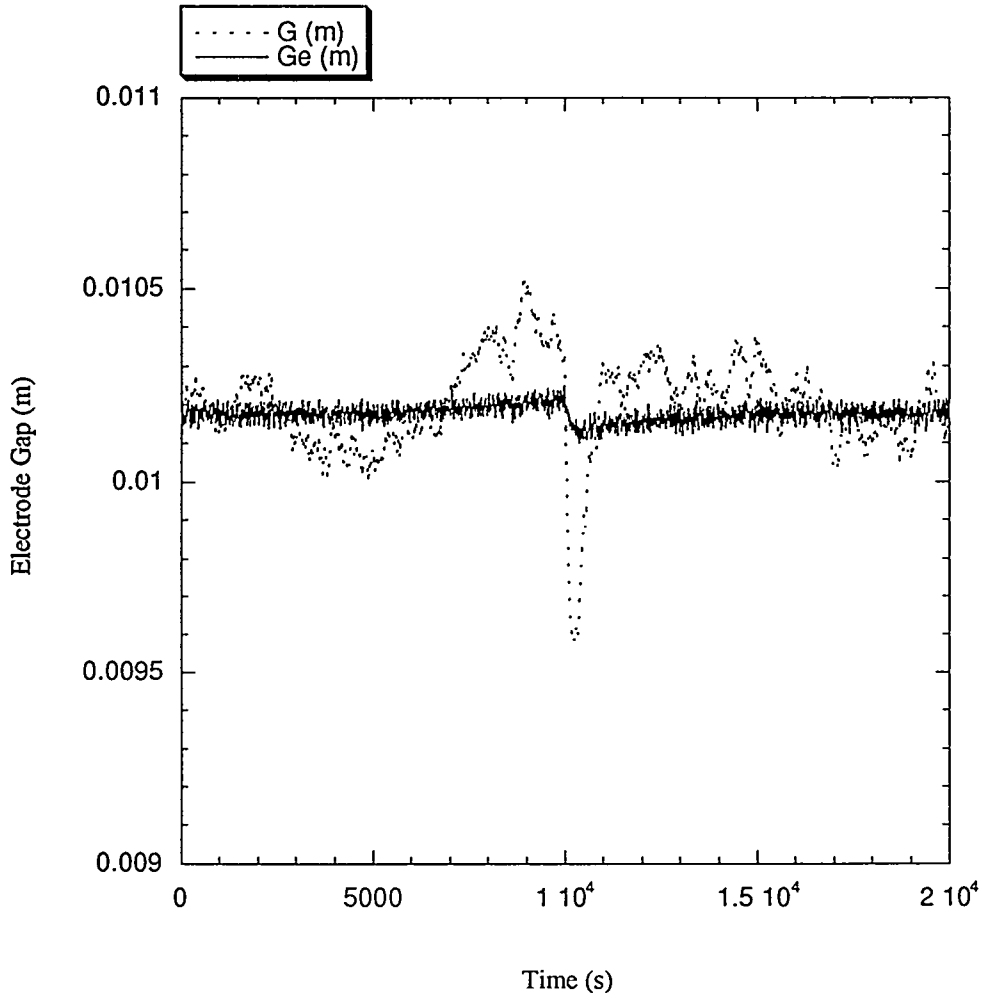

Figure 7. Plot showing the closed-loop controller output for the simulated melt rate event using the same gains as were used to generate the open-loop data shown in Figure 5.

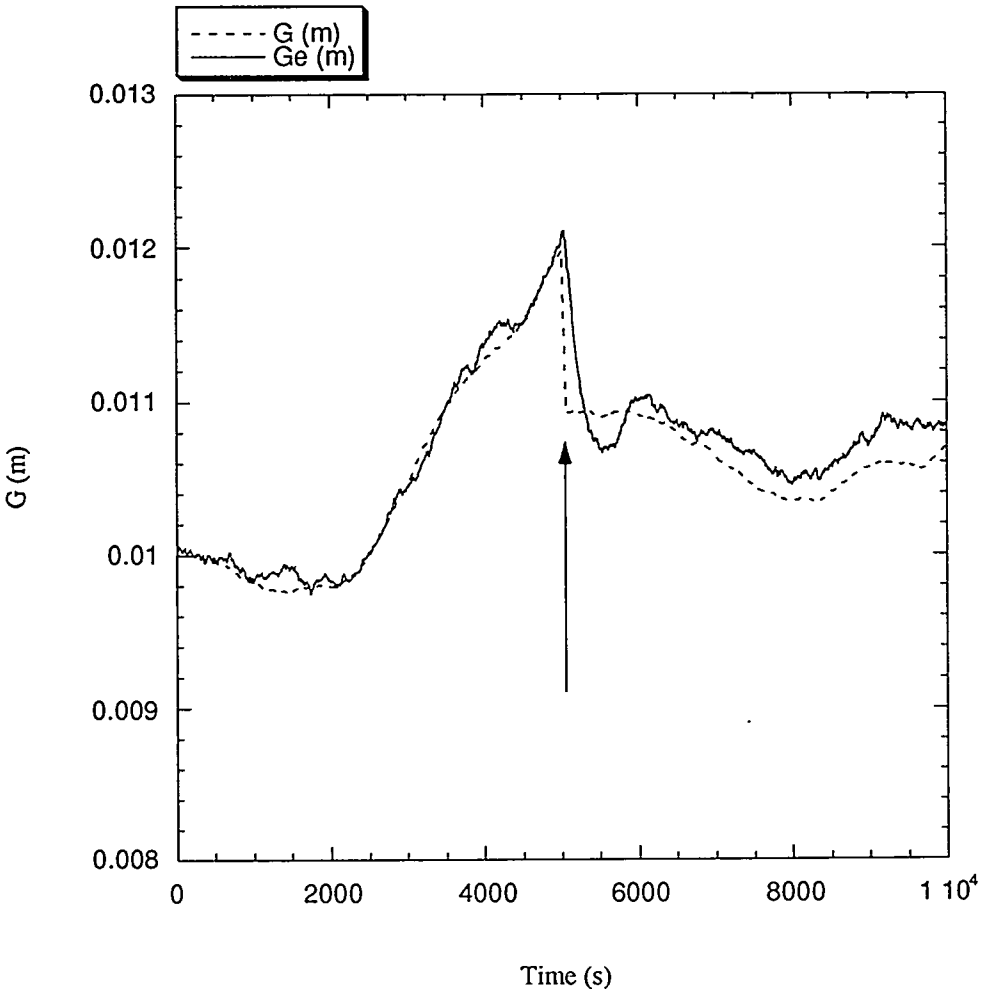

Figure 8. Plot showing the open-loop estimated electrode gap and the true gap during the simulated glow condition. The glow begins at t=5000 s (arrow) and ends 60 s later.

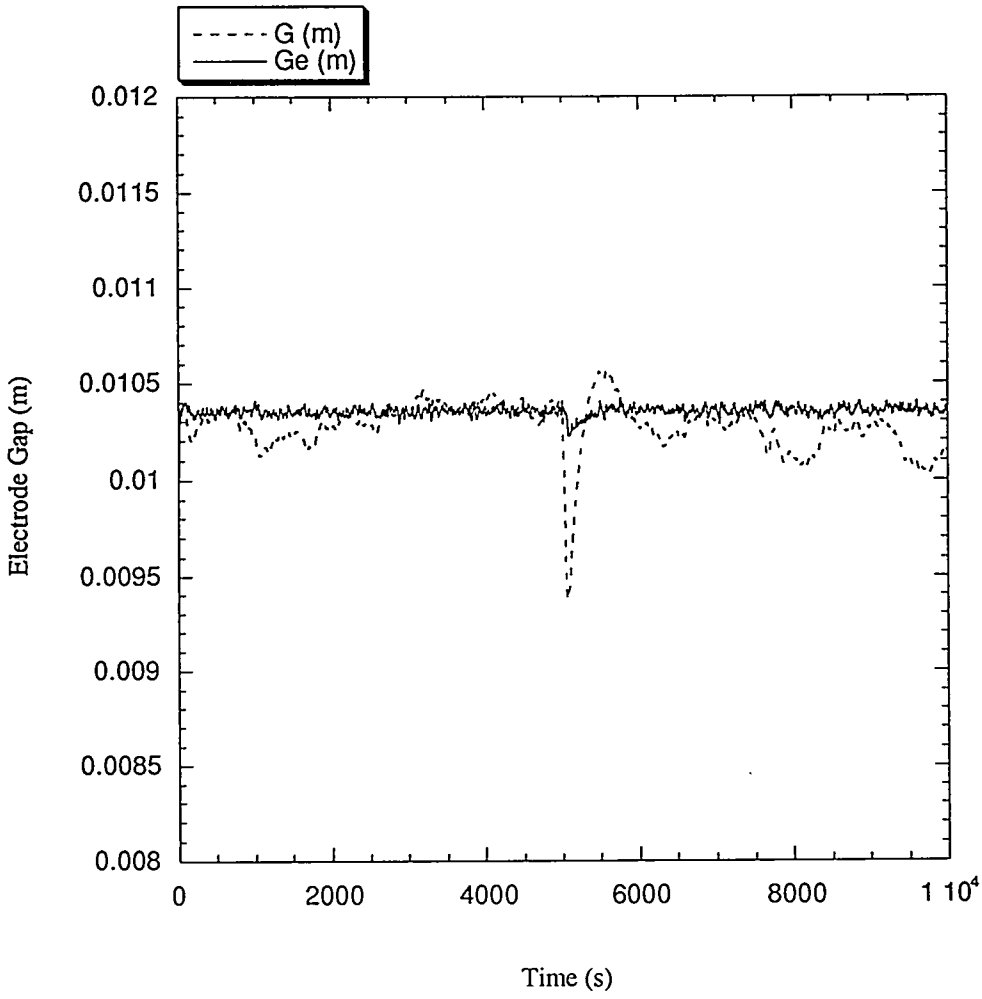

Figure 9. Plot showing the closed-loop controller output for the simulated glow condition with the same gain settings as were used to produce the results shown in Figure 8.

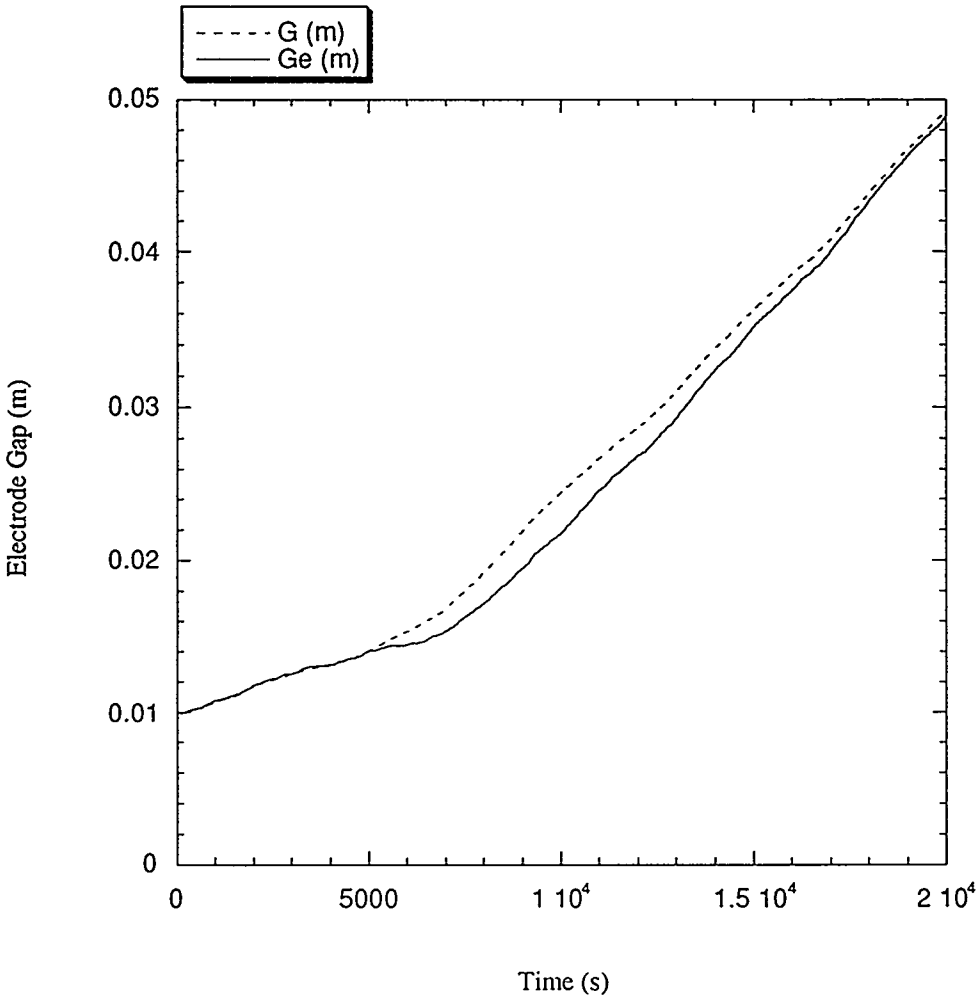

Figure 10. Plot showing the open-loop response to a –0.005 m bias in the electrode gap measurement. The bias was applied at t=5000 s and ended at t=10,000 s.

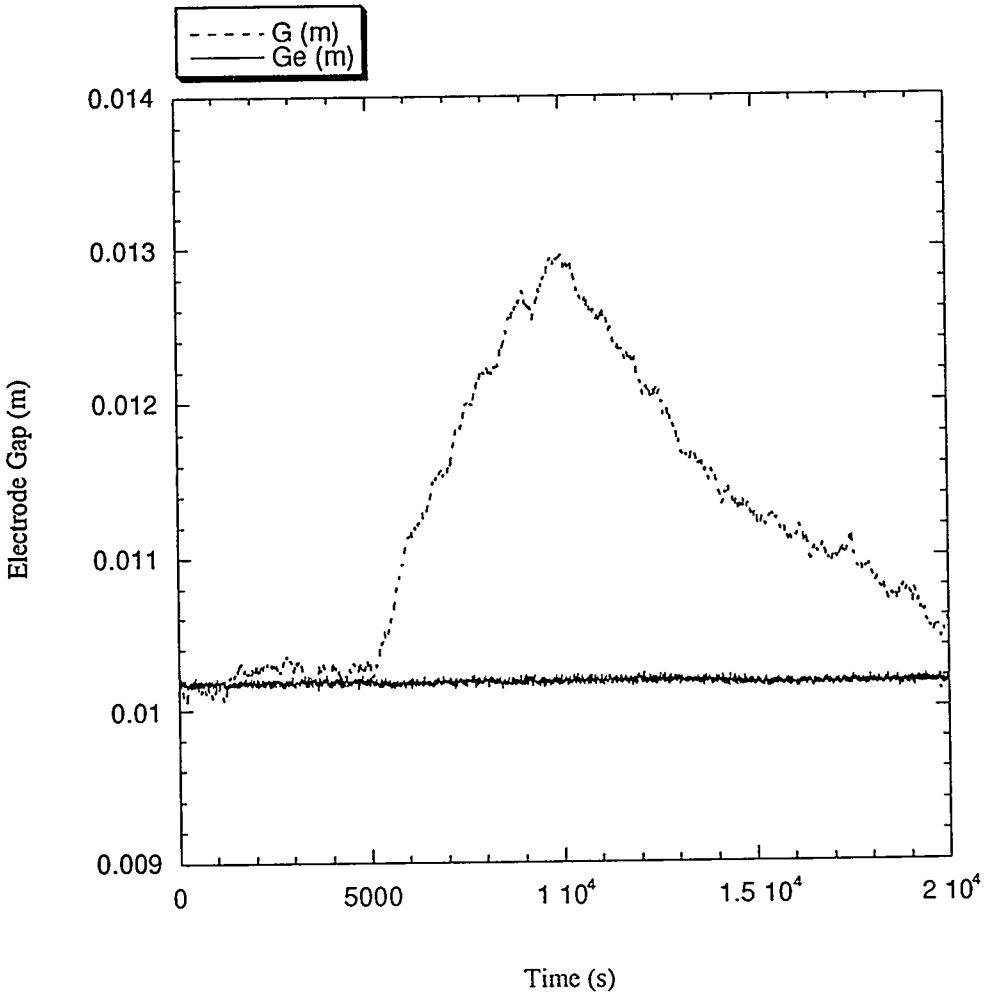

Figure 11. Plot showing the closed loop response to the disturbance of Figure 10 with the same gains.

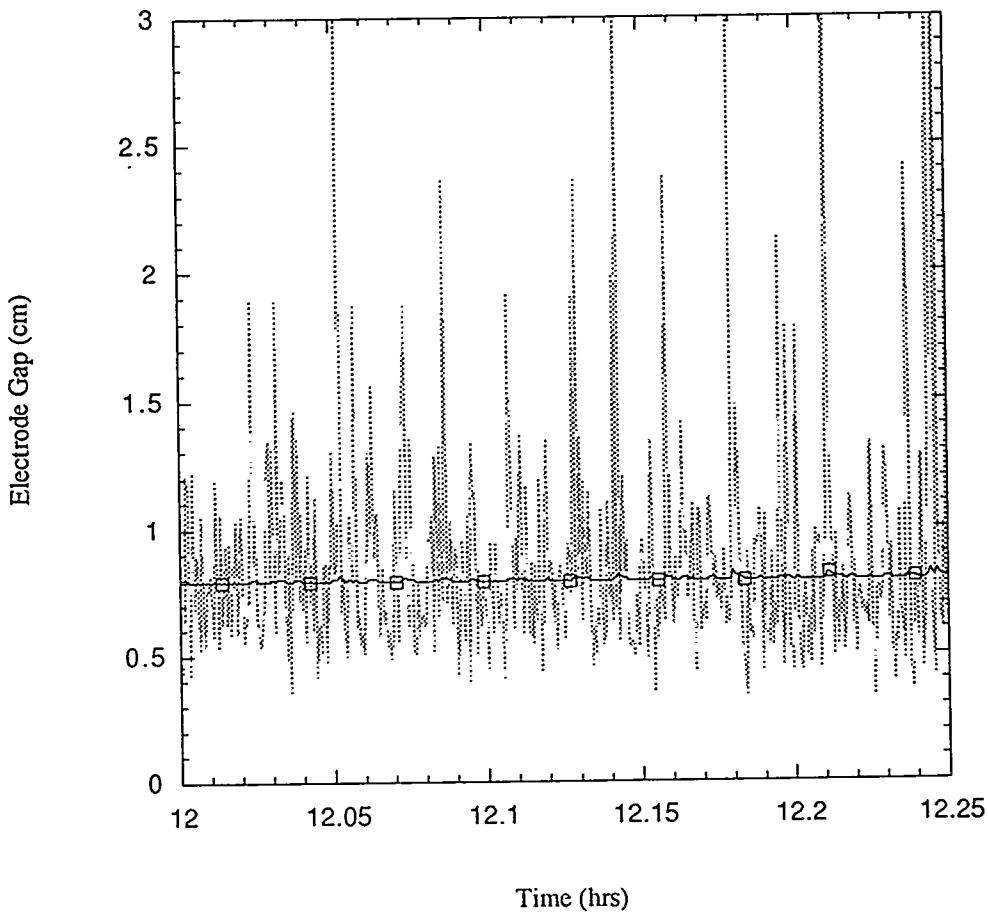

Figure 12. Sample data during VAR of Alloy 718 melting at approximately 0.040 kg/s showing the Kalman filtered gap estimate and the estimate based solely on drip-short data over two second intervals. Control decisions were based on the filtered estimates.